Supplementary Information

Altered MCM Protein Levels and Autophagic Flux in Aged and Systemic Sclerosis Dermal Fibroblasts

Verónica I. Dumit, Victoria Küttner, Jakob Käppler, Sonsoles Piera-Velazquez, Sergio A. Jimenez, Leena Bruckner-Tuderman, Jouni Uitto and Jörn Dengjel

Supplementary Figures

Supplementary Figure 1	Histograms representing age-dependent proteomal changes.
Supplementary Figure 2	Immunostaining against MCM7.
Supplementary Figure 3	Immunoblots against LC3 to determine autophagic fluxes of fibroblasts of donors of different ages.
Supplementary Figure 4	Immunostaining against LC3 of healthy fibroblasts of donors of different ages.
Supplementary Figure 5	Correlation between MS replicates.
Supplementary Figure 6	Immunoblots against LC3 to determine autophagic fluxes in SSc fibroblasts.
Supplementary Figure 7	Immunostaining against LC3 in SSc and control cells.
Supplementary Figure 8	Immunostaining against LC3 in MCM7 knock-down and control fibroblasts.

Supplementary Tables

Supplementary Table 1	Proteome of skin fibroblasts from different donors of different ages: 0, 4, 14, 20 and 33 years.
Supplementary Table 2	Enriched GO terms in clusters with age-dependent increase or decrease of protein abundance.

Supplementary Figures

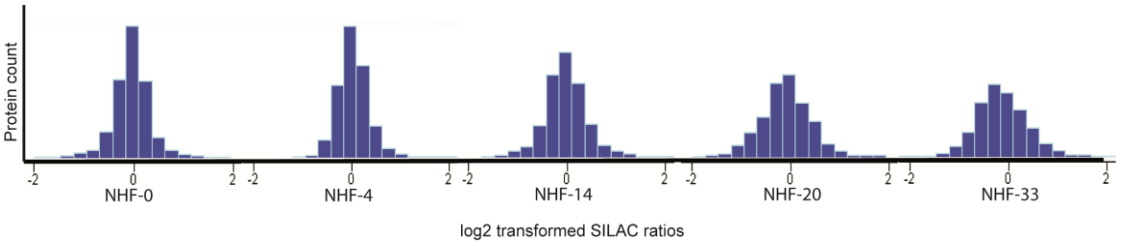

Figure 1: Histograms representing proteome changes of fibroblasts from donors of ages 0, 4, 14, 20 and 33 years compared to the internal standard.

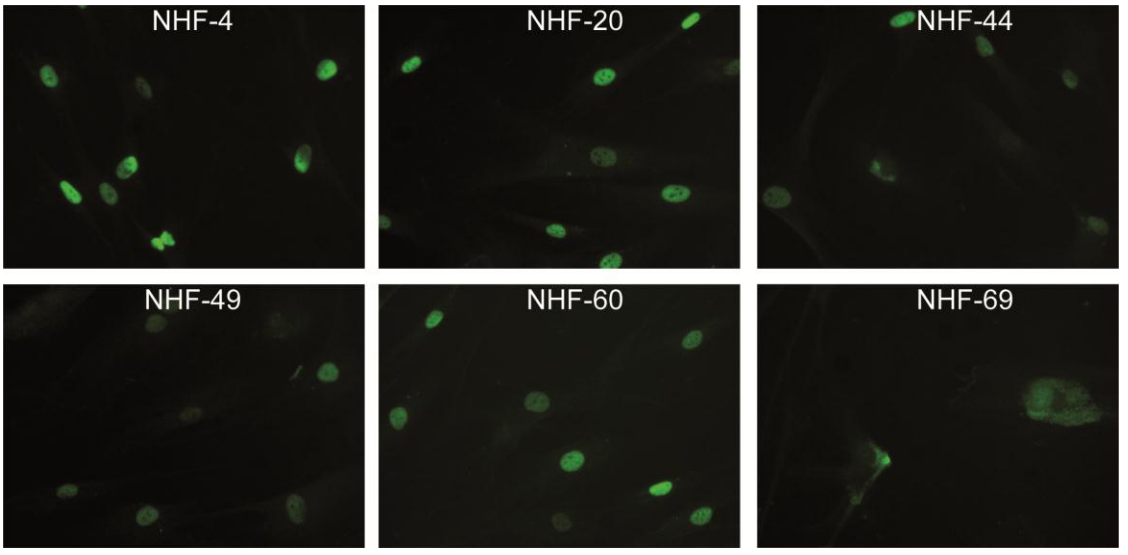

Figure 2: Microscopy pictures of MCM7 immunostainings of cells of different ages. A shift in subcellular localization can be observed, older cells having more MCM7 in the cytosol.

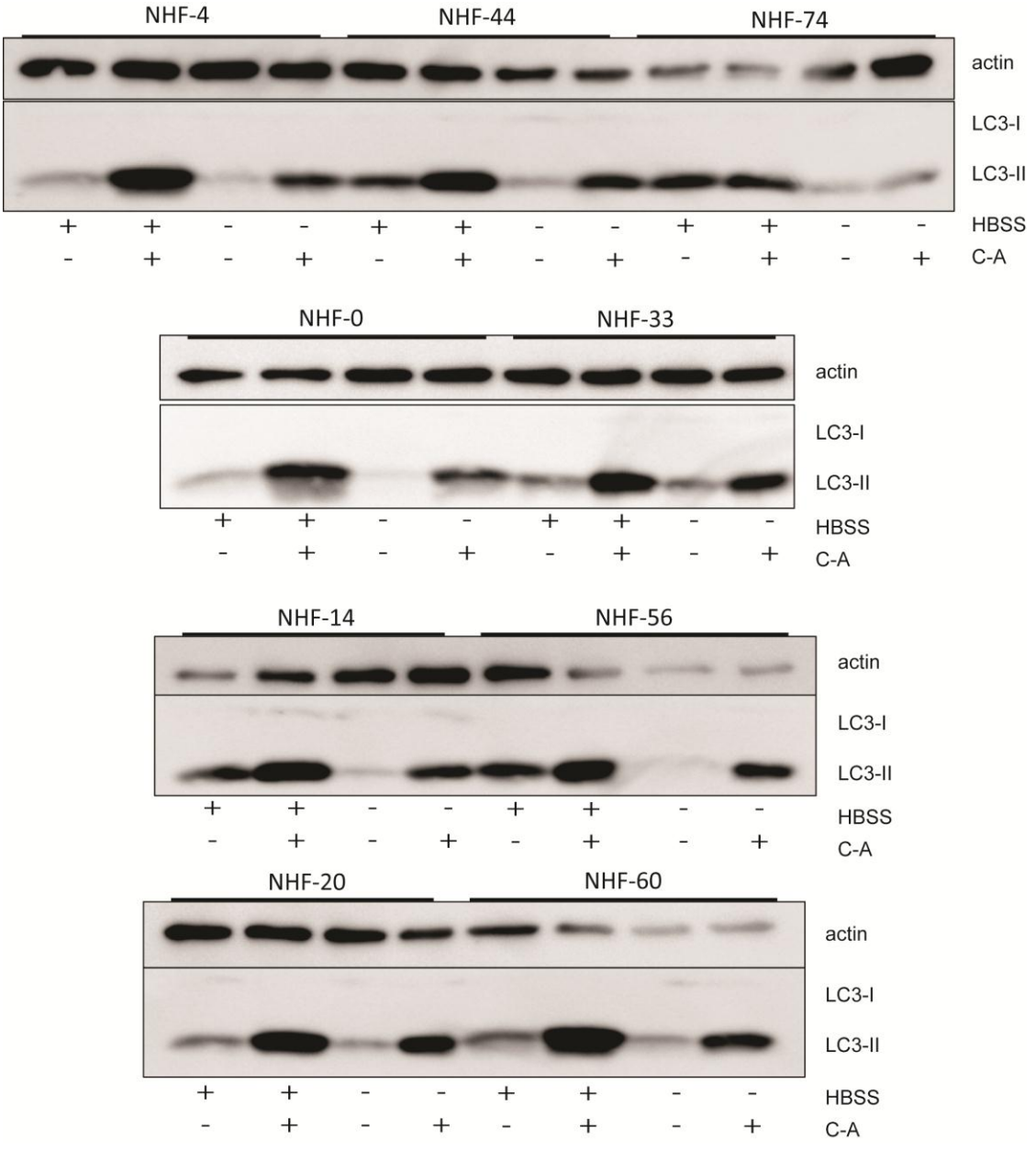

Figure 3: Immunoblots against LC3 to determine autophagic fluxes under amino acid starvation (HBSS) and control conditions. Quantification is shown in Figure 2. Actin was used as loading control.

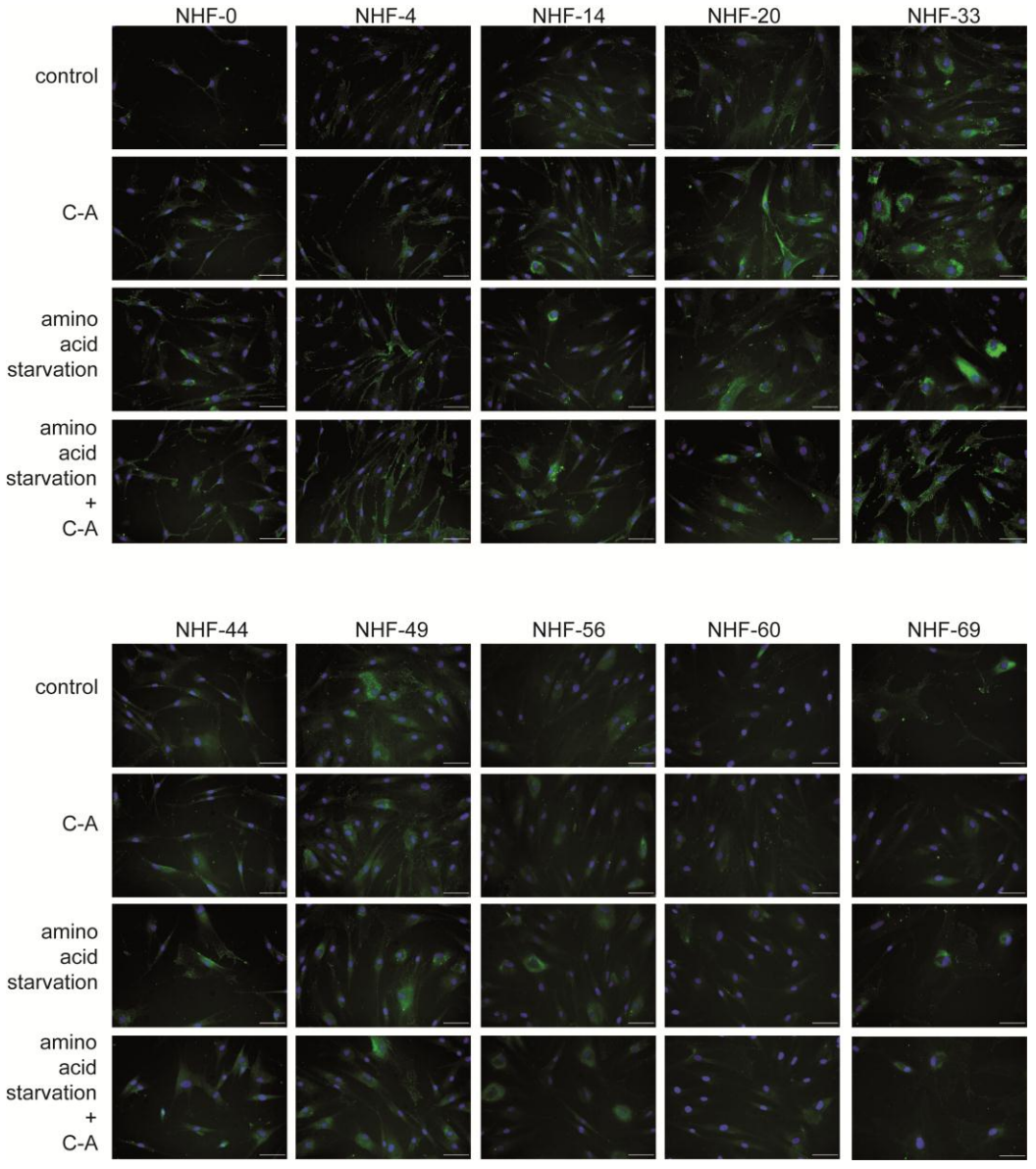

Figure 4: Microscopy pictures of LC3 immunostainings of cells of different ages, under four different treatments: control, C-A, amino acid starvation, and amino acid starvation plus C-A. An accumulation of LC3 in older cells and a decrease in responsiveness to starvation can be observed.

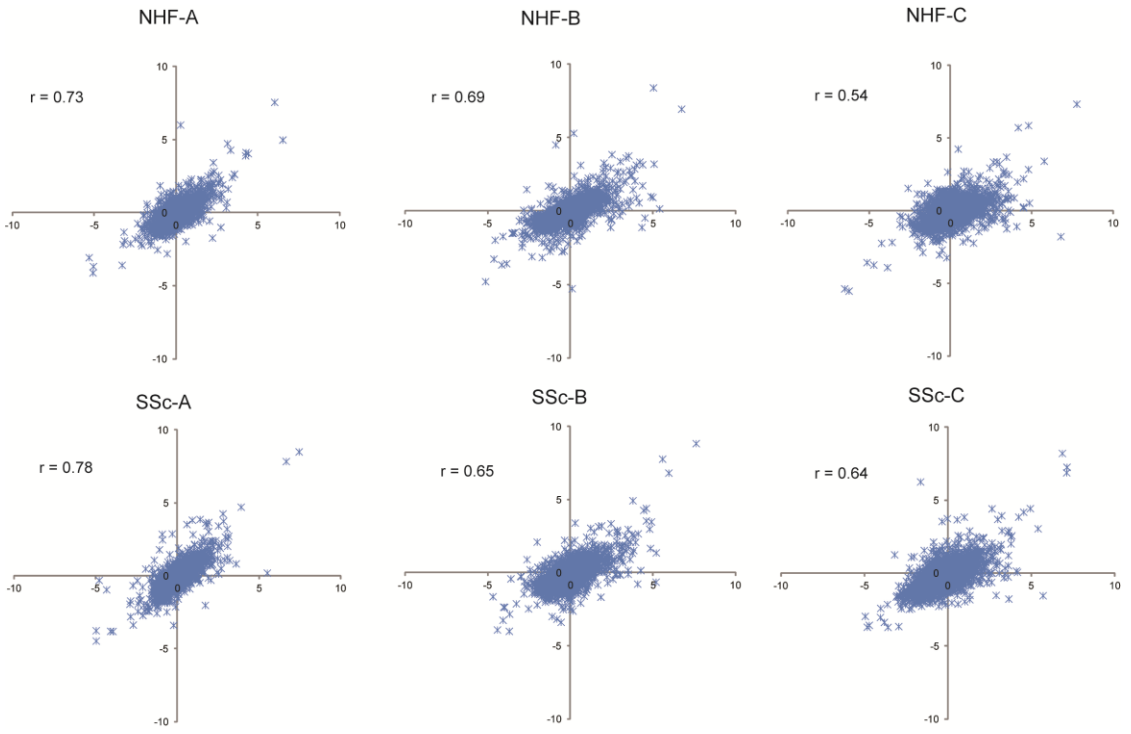

Figure 5: Correlation between two biological replicates of SSc fibroblast proteomes measured by mass spectrometry, plotted as $\log_2$ transformed SILAC ratios of respective experiments.

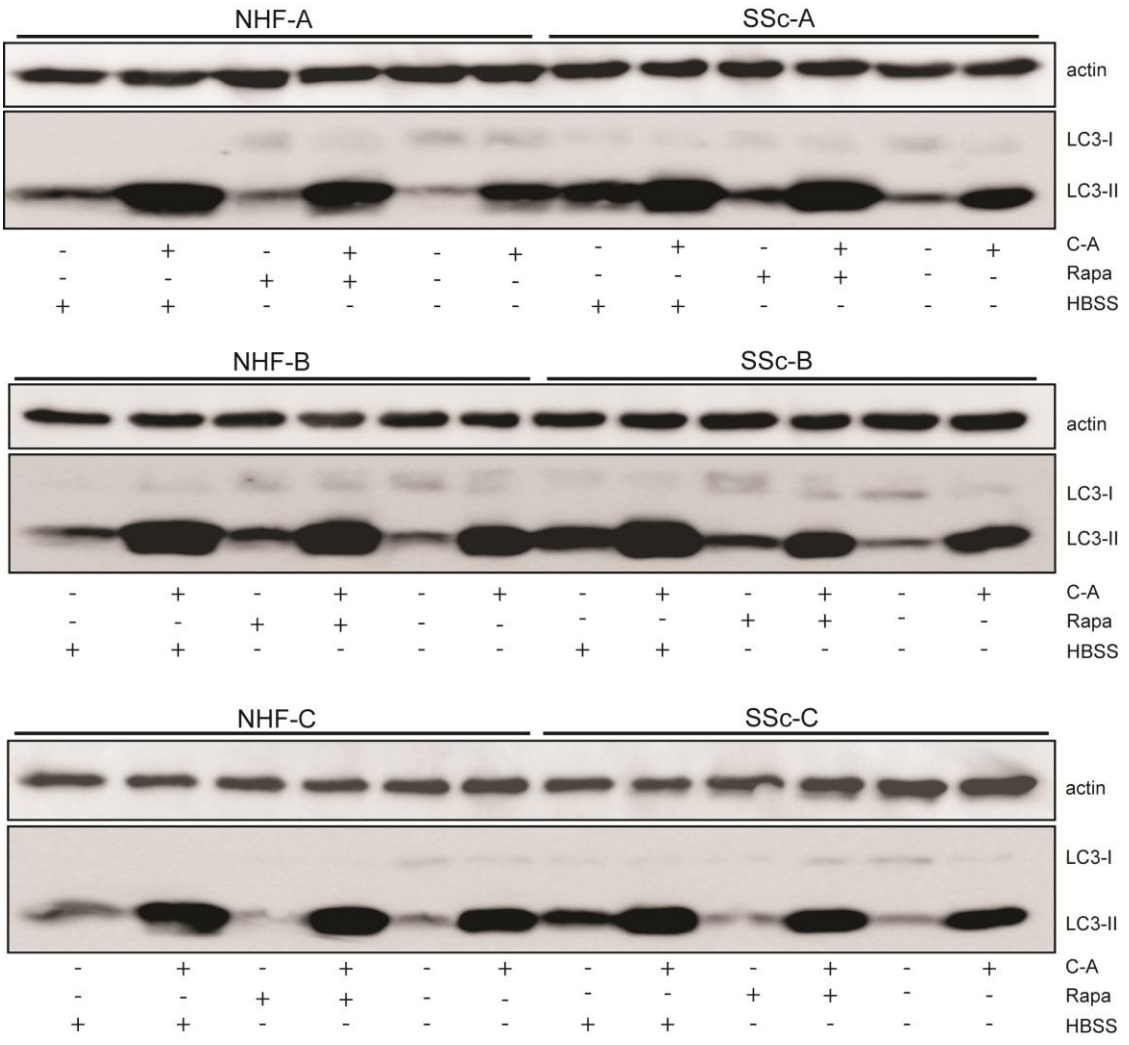

Figure 6: Immunoblots against LC3 to determine autophagic fluxes under amino acid starvation (HBSS), rapamycin (Rapa) and control conditions. Quantification is shown in Figure 4. Actin was used as loading control.

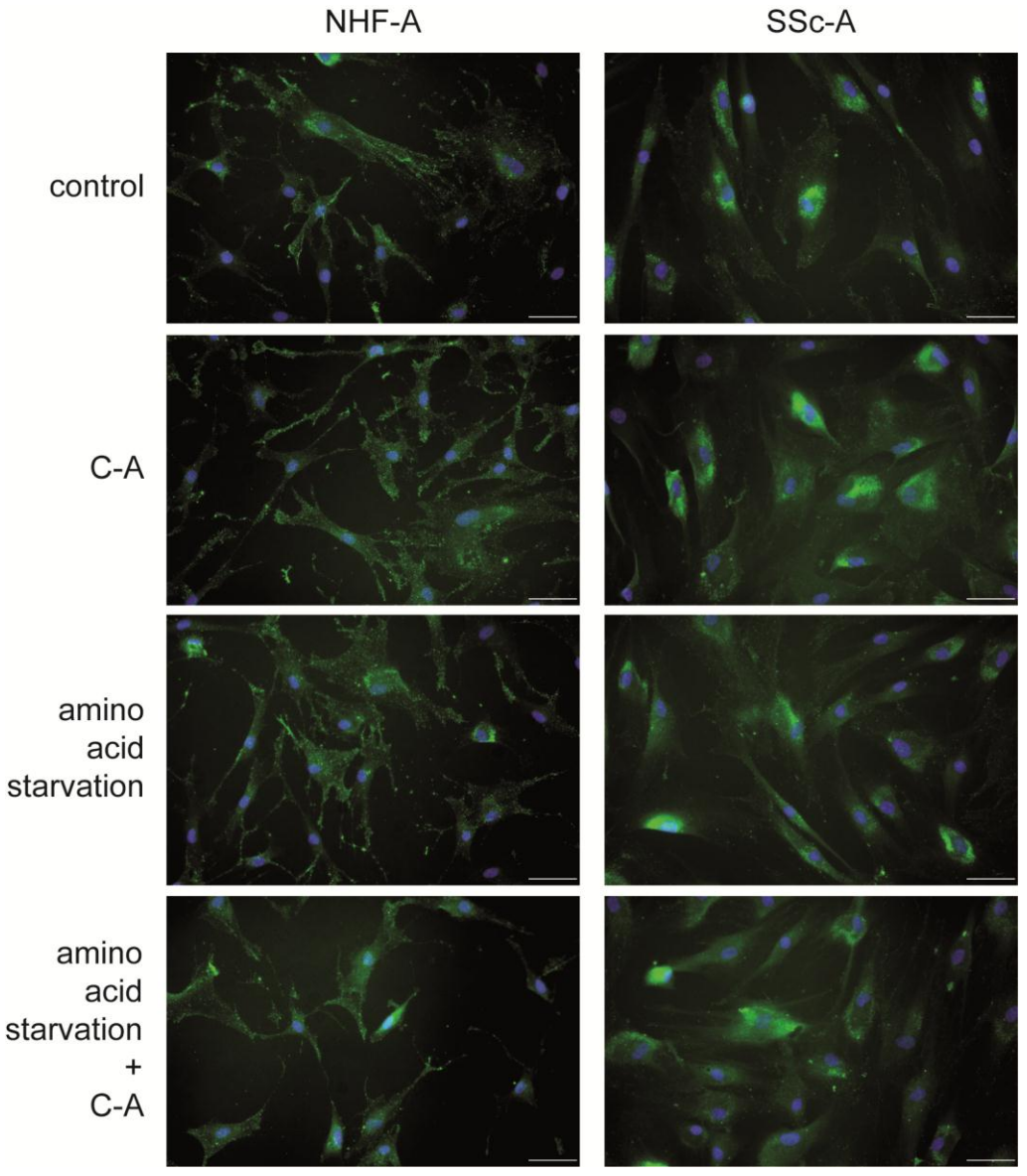

Figure 7: Microscopy pictures of LC3 immunostainings of SSc and control fibroblasts, under four different treatments: control, C-A, amino acid starvation, and amino acid starvation plus C-A. An accumulation of LC3 in SSc cells and a decrease in responsiveness to starvation can be observed.

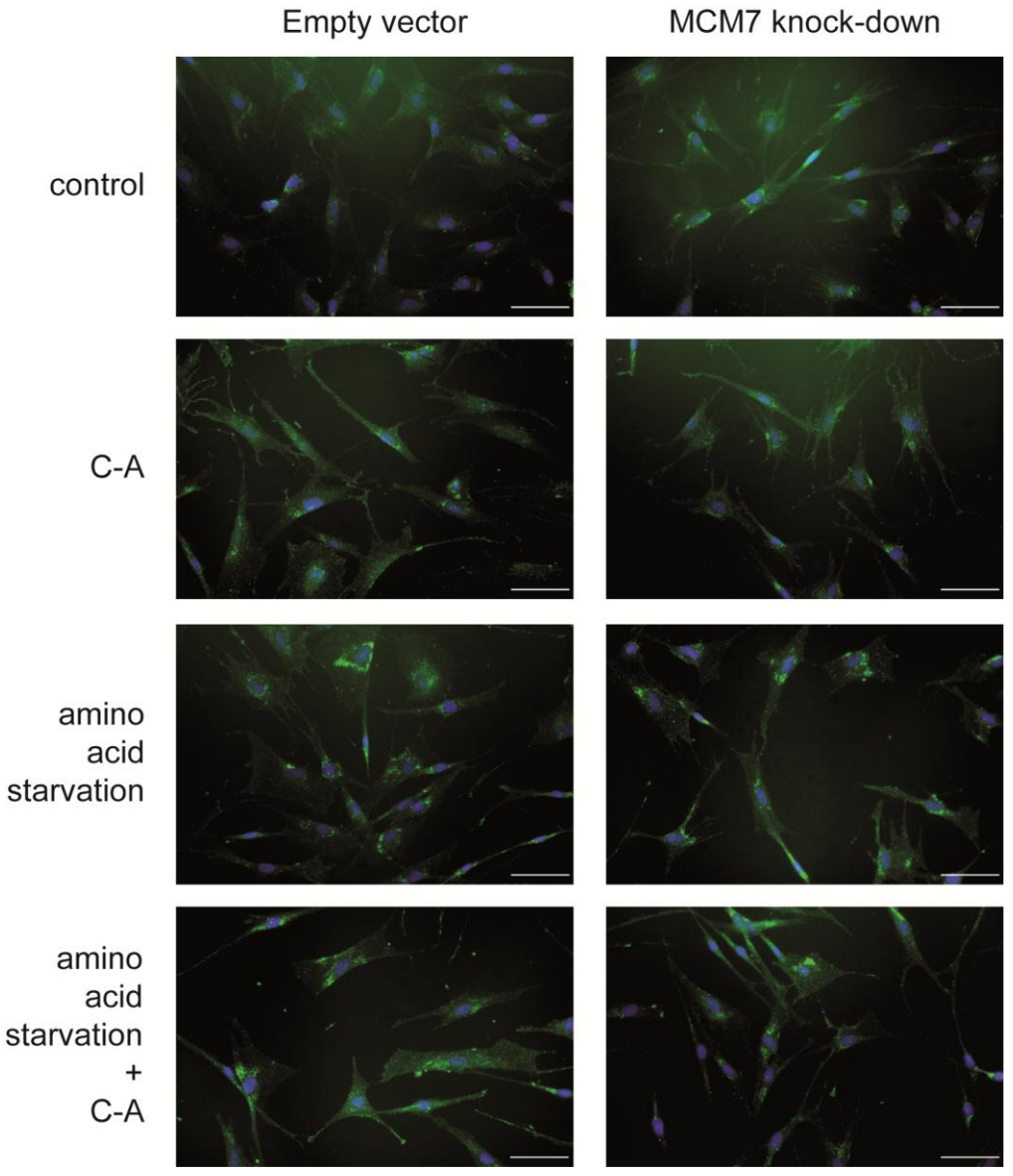

Figure 8: Microscopy pictures of LC3 immunostainings of MCM7 knock-down and control fibroblasts, under four different treatments: control, C-A, amino acid starvation, and amino acid starvation plus C-A. An accumulation of LC3 in knock-down cells and a decrease in responsiveness to starvation can be observed.

Materials & Methods

Cell types.

The study was approved by the Ethics Committees of Jefferson Medical College and Freiburg University and conducted according to the Declaration of Helsinki. All included patients gave that their written, informed consent. All SSc biopsies were taken from the forearm of patients with an active, early-diffuse form of the disease. The different fibroblast types included in the experiment are described in Table 1 of the main text. With the aim to characterize the aging phenotype of skin fibroblasts, we used NHF taken from non-sun-exposed skin of healthy donors.

Mass spectrometry sample preparation and measurements.

Harvested cells were resuspended in lysis buffer (100 mM Tris pH 7.6; 4% SDS supplemented with protease inhibitor cocktail). Benzonase was added before reducing the samples with 1 mM DTT for 5 min at 95^{o}C and alkylated using 5.5 mM iodacetamide for 30 min at 25^{o}C. Protein mixtures were separated by SDS-PAGE (4-12% Bis-Tris mini gradient gel), gel lanes were cut into 10 equal slices, and in-gel digested using trypsin (Shevchenko et al., 2006). Resulting peptide mixtures were processed on STAGE tips as described (Rappsilber et al., 2007).

Samples analyzed by MS were measured on LTQ Orbitrap XL mass spectrometer (Thermo Fisher Scientific, Bremen, Germany) coupled either to an Agilent 1200 nanoflow-HPLC (Agilent Technologies GmbH, Waldbronn, Germany) or an Eksigent

NanoLC-ultra. HPLC-column tips (fused silica) with 75 μm inner diameter were self-packed (Gruhler et al., 2005) with Reprosil-Pur 120 ODS-3 to a length of 20 cm. No pre-column was used. Peptides were injected at a flow of 500 nl/min in 92% buffer A (0.5% acetic acid in HPLC gradient grade water) and 2% buffer B (0.5% acetic acid in 80% acetonitrile, 20% water). Separation was achieved by a linear gradient from 10% to 30% of buffer B at a flow rate of 250 nl/min. The mass spectrometer was operated in the data-dependent mode and switched automatically between MS (max. of 1 x10 ions) and MS/MS. Each MS scan was followed by a maximum of five MS/MS scans in the linear ion trap using normalized collision energy of 35% and a target value of 5,000. Parent ions with a charge states of z = 1 and unassigned charge states were excluded from fragmentation. The mass range for MS was m/z = 370 to 2,000. The resolution was set to 60,000. MS parameters were as follows: spray voltage 2.3 kV; no sheath and auxiliary gas flow; ion transfer tube temperature 125°C.

Data analysis.

The MS raw data files were uploaded into the MaxQuant software version 1.2.18 (Cox and Mann, 2008) which performs peak and SILAC-pair detection, generates peak lists of mass error corrected peptides and data base searches. A full length IPI human database containing common contaminants, such as keratins and enzymes used for in-gel digestion, (based on IPI human version 3.68) was employed, carbamidomethylcysteine was set as fixed modification and methionine oxidation and protein amino-terminal acetylation were set as variable modifications. Double SILAC

was chosen as quantitation mode. Three miss cleavages were allowed, enzyme specificity was trypsin/P+DP, and the MS/MS tolerance was set to 0.5 Da. The average mass precision of identified peptides was in general less than 1 ppm after recalibration. Peptide lists were further used by MaxQuant to identify and relatively quantify proteins using the following parameters: peptide, and protein false discovery rates (FDR) were set to 0.01, maximum peptide posterior error probability (PEP) was set to 0.1, minimum peptide length was set to 6, minimum number peptides for identification and quantitation of proteins was set to two of which one must be unique, and identified proteins have been re-quantified. The "match-between-run" option (2 min) was used.

For the generation of the heat map by Perseus (Cox and Mann, 2008), samples were ordered according to age and proteins were hierarchically clustered using Euclidian Distance as matrix ($\log_2$ transformed and z normalized SILAC protein ratios). To address the biological implications of the proteins in each cluster, Gene Ontology terms were retrieved and tested for enrichment compared to the remainder of the dataset using the Fishers' exact test ($p<0.05$). DAVID 6.7 BETA (Huang et al., 2009b, 2009a) was used to detect deregulated pathways using GO annotation and functional annotation clustering, with the default settings with a minimum significance of $p<0.05$.

Protein concentration determination.

$8\ 10^5$ cells were seeded per 10 cm plate and harvested the next day using a cell scraper. Harvested cells were lysed with 80 µL of lysis buffer, incubated for 20 min with benzonase, and centrifugated at 16.000 rcf during 15 min. Supernatant was used for

determination of protein concentration employing the Thermo Scientific Pierce BCA Protein Assay Kit as recommended by the supplier.

Determination of cell proliferation rates.

8 10^5 fibroblasts per 10 cm plate were seeded and counted every two days using a onetime heamocytometer (Glasstic slide) with 8 µL of suspension of cells. Counted cells were seeded in a new plate and recounted over 40 days. The data of the first 8 days of experiment were used to calculate the proliferation rates.

Immunofluorescence staining.

For indirect immunofluorescence staining, fibroblasts grown on cover slips were fixed with 4% PFA and blocked with 2% BSA in PBS for 30 min at room temperature, followed by incubation with the primary antibody diluted in 0.2% BSA in PBS for 1 hour at room temperature. After incubation with the secondary antibody in 0.2% BSA in PBS for 1 hour, the samples were embedded in DAPI containing fluorescence mounting medium (ProLong® Gold, Invitrogen, Darmstadt, Germany). The following primary antibodies were used: anti-MCM7 (AB2360, Abcam, Cambridge, United Kingdom) and anti-LC3 (clone5F10, Nanotools, Teningen, Germany). Alexa488–conjugated secondary antibodies (Invitrogen, Darmstadt, Germany) were used. Pictures were taken with an IF microscope (Zeiss Axio Imager, Zeiss, Oberkochen, Germany).

β-Galactosidase activity staining.

For detection of β-galactosidase activity a commercial kit was used as recommended by

the supplier (β-galactosidase activity kit from Cell Signalling).

Supplementary References

Cox, J. and Mann, M. (2008). Maxquant enables high peptide identification rates, individualized p.p.b.-range mass accuracies and proteome-wide protein quantification. *Nat Biotechnol*, 26:1367–1372.

Gruhler, A., Olsen, J. V., Mohammed, S., et al. (2005). Quantitative phosphoproteomics applied to the yeast pheromone signaling pathway. *Mol Cell Proteomics*, 4:310–327.

Huang, d. a. W., Sherman, B. T., and Lempicki, R. A. (2009a). Bioinformatics enrichment tools: paths toward the comprehensive functional analysis of large gene lists. *Nucleic Acids Res*, 37:1–13.

Huang, d. a. W., Sherman, B. T., and Lempicki, R. A. (2009b). Systematic and integrative analysis of large gene lists using DAVID bioinformatics resources. *Nat Protoc*, 4:44–57.

Martins, V. L., Vyas, J. J., Chen, M., et al. (2009). Increased invasive behaviour in cutaneous squamous cell carcinoma with loss of basement-membrane type vii collagen. *J Cell Sci*, 122:1788–1799.

Rappsilber, J., Mann, M., and Ishihama, Y. (2007). Protocol for micro-purification, enrichment, pre-fractionation and storage of peptides for proteomics using StageTips. *Nat Protoc*, 2:1896–1906.

Shevchenko, A., Tomas, H., Havlis, J., et al. (2006). In-gel digestion for mass spectrometric characterization of proteins and proteomes. *Nat Protoc*, 1:2856–2860.